Journal of Computational Science 73 (2023) 102138

Contents lists available at ScienceDirect

Journal of Computational Science

journal homepage: www.elsevier.com/locate/jocs

A study of the potential effects of deepening the Corpus Christi Ship Channel on hurricane storm surge

Eirik Valseth [a,c,d,*], Clint Dawson [a], Edward Buskey [b]

[a] The Oden Institute for Computational Engineering and Sciences, The University of Texas at Austin, 201 E. 24th St. Stop C0200, Austin, 78712, TX, United States of America
[b] The Marine Science Institute, The University of Texas at Austin, 750 Channel View Drive, Port Aransas, 78373, TX, United States of America
[c] The Department of Data Science, The Norwegian University of Life Science, Drøbakveien 31, Ås, 1433, Norway
[d] Department of Scientific Computing and Numerical Analysis, Simula Research Laboratory, Kristian Augusts gate 23, Oslo, 0164, Norway

ARTICLE INFO

Keywords:
ADCIRC
Storm surge
Hurricane harvey
Channel deepening

ABSTRACT

We present a case study of the potential impact on hurricane storm surge due to deepening the Corpus Christi Ship Channel through Aransas Pass in the region of Corpus Christi and Port Aransas, Texas. Our investigation is based on numerical mathematical models of the circulation of coastal water due to Hurricane Harvey and a synthetic hurricane derived from Harvey. The circulation models are based on the numerical solution of the shallow water equations using finite element and finite difference techniques. The shallow water equations are solved within the framework of the widely used ADvanced CIRCulation (ADCIRC) numerical model. From the models, we ascertain maximum storm surge as well as elevation time series at critical locations in the study region. To assess the effects of a deeper channel, we compare the model outputs for current and proposed future channels. The model results indicate that the changes to maximum storm surge magnitude are small and in large portions of the study area the models indicate a reduction in surge magnitude. However, there are some local areas where the models results show an increase of up to 30 centimeters in a synthetic extreme storm scenario.

1. Introduction

The Corpus Christi ship channel extends from the Gulf of Mexico to the port of Corpus Christi through Corpus Christi Bay and Aransas Pass [1]. The location of the channel is shown in Figs. 1 and 2, where the channel is seen as the dark blue areas through Corpus Christi bay in Fig. 2. The current channel configuration was established in 1989 and has an average depth of 14.33 m (47 ft), which is maintained through a continuous dredging operation [1]. The channel allows commercial vessels to enter and exit the system of bays to reach the port of Corpus Christi through the Aransas Pass which is the only nearby remaining natural tidal inlet. Inside the Aransas Pass there are several shallow bays and regions that are of both recreational and commercial interest due to multiple fish species. Additionally, these estuary systems are important recreational areas for the population in the region.

To accommodate growth and expansion of the activities of the Port of Corpus Christi, it has been proposed to deepen the ship channel through the pass to 21.33 m (70 ft). This is proposed to accommodate ships with larger freight and shipping capacity at the port. A deeper ship channel is likely to affect the flow characteristics of the seawater that enters and exits Aransas Pass and in the bays behind it. In a previous study, we investigated the impact of a deeper channel on passive Lagrangian particle transport of Red Drum fish larvae [2]. While the flow pattern and velocity of the seawater through Aransas Pass was changed in a significant manner, the transport of Red Drum larvae was only marginally impacted.

The Texas coastline near Corpus Christi is frequently impacted by hurricanes and smaller storms leading to often damaging storm surges, see [3] for a review of some of these. In August 2017, the study area shown in Fig. 2 was significantly impacted by Hurricane Harvey which produced significant surge in the City of Port Aransas. The winds that occurred during this hurricane lead to significant surge from the winds directed towards the shoreline in addition to surge within Corpus Christi Bay from its alongshore winds [4]. Based on findings in our previous study, we now study the effects of a deeper channel on hurricane storm surge in the region. To this end, we develop two distinctive circulation models, one for the current channel and another for the proposed deeper channel. As Hurricane Harvey lead to significant surges in large parts of the study area, we consider Hurricane Harvey and a synthetic hurricane. The synthetic hurricane is based on

* Corresponding author at: The Department of Data Science, The Norwegian University of Life Science, Drøbakveien 31, Ås, 1433, Norway.
E-mail address: eirik.valseth@nmbu.no (E. Valseth).

https://doi.org/10.1016/j.jocs.2023.102138
Received 31 May 2023; Received in revised form 1 August 2023; Accepted 25 August 2023
Available online 9 September 2023

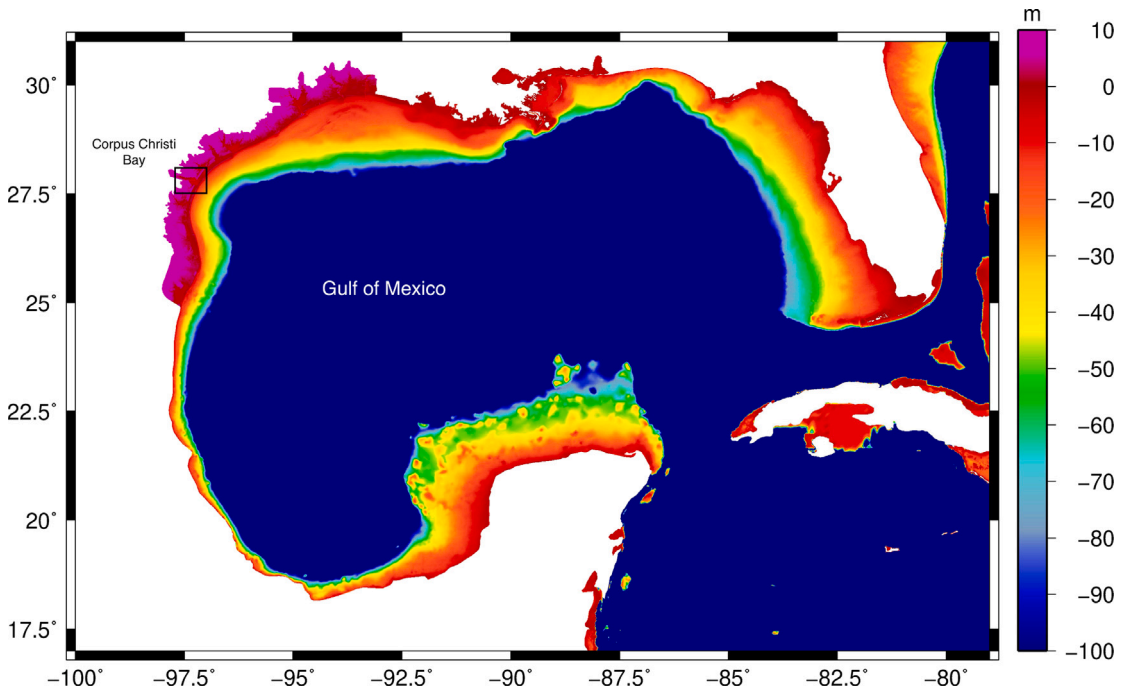

Fig. 1. Map of the Gulf of Mexico with study area highlighted. The color indicates the bathymetry, with areas deeper than 100 meter shown as dark blue..

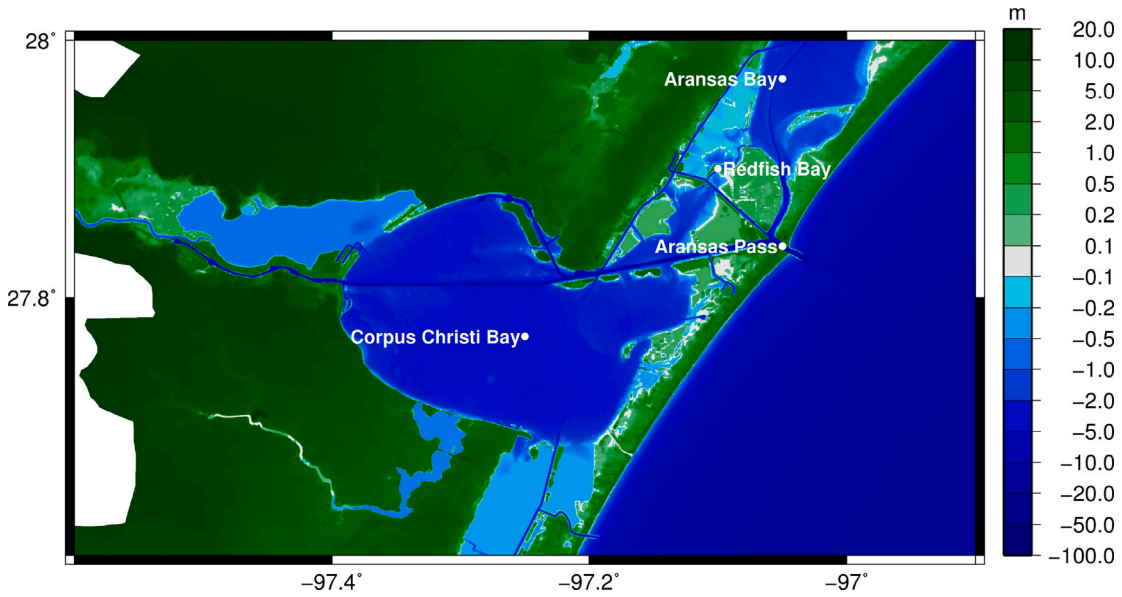

Fig. 2. Study area near Corpus Christi.

the wind and pressure fields of Harvey. However, the track is shifted to increase the storm surge through Aransas Pass. From the models, we ascertain both sea surface elevation and the flow velocity field for the entire model domain and time span of consideration. However, we focus on the elevation and in particular the maximum modeled elevation.

Case studies of the impacts of channel deepening has been studied by multiple researchers in the past. Some works include our own aforementioned study of fish larvae transport [2], effects on sediment transport [5], coastal erosion [6], and storm surge [7–10]. In [7], the effects of deepening the St. Johns River, Florida, on storm surge, mean low water, mean high water, and sea level rise were considered by numerical modeling using the ADvanced CIRculation (ADCIRC) model [11]. It was found that the deepening of the St. Johns River (up to 3m) did not significantly alter the magnitude and extent of storm surge but some localized areas saw changes up to 15 cm. In [8], the impacts of channel deepening is studied by modeling an idealized inlet followed by Delft3D [12] model runs of variable storm intensity, tidal constituents, storm timing, and storm track. In this work, it is shown that the storm surge in the Cape Fear River Estuary, Wilmington, North Carolina, may be significantly increased due to its significantly deepened bathymetry over the past century. In [9], a simplified analytic model for an idealized inlet is developed and used to study the interaction between surges and tides.

In the following, we describe the modeling methodology we employed in Section 2. In Section 3, we present the outputs from the developed models and compare the results based on current and proposed channel depths for the storms considered. Last, in Section 4 we

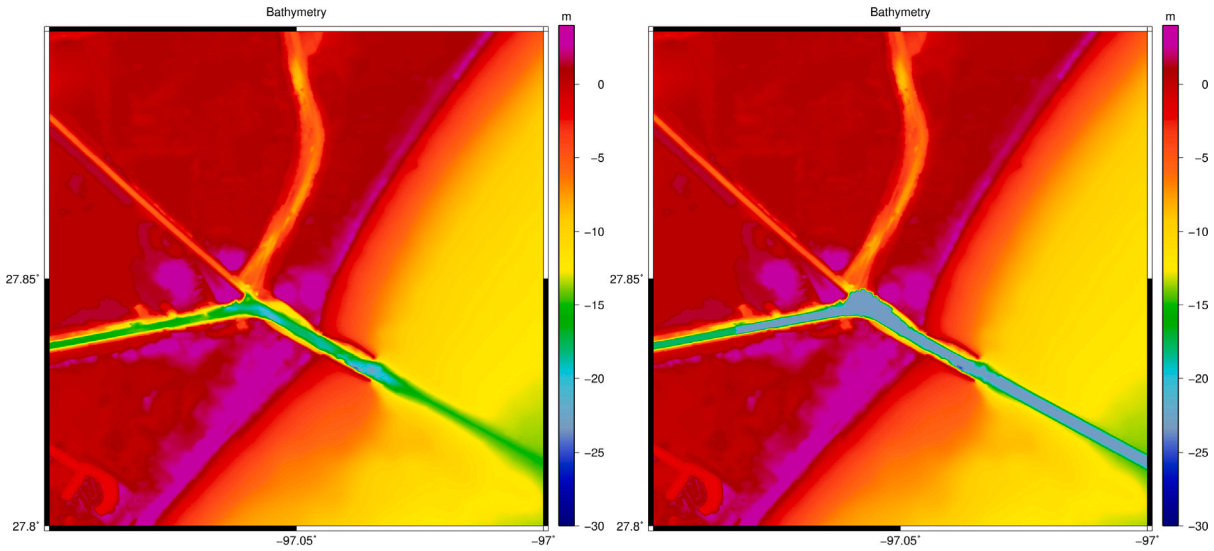

(a) Existing. (b) Proposed.

Fig. 3. Bathymetry near the Aransas Pass.

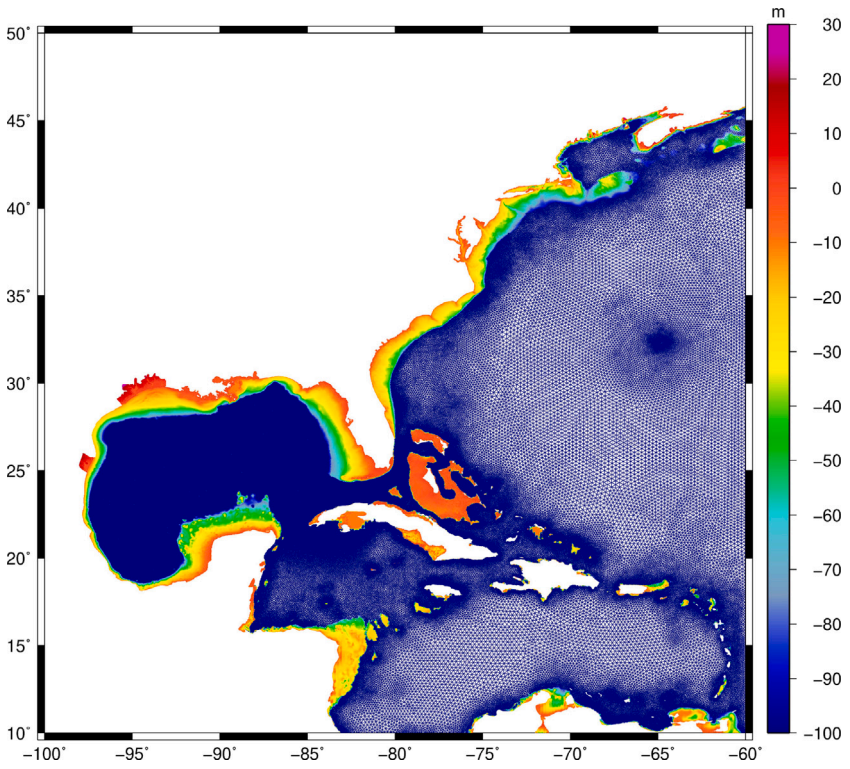

Fig. 4. Model domain covered by the ADCRIC finite element mesh. Note that the bathymetry measured in meters cut off at 100 m.

draw conclusions and propose future directions of study and research. Note that in the following, we use the term "bathymetry" for the depth of water relative to the North American Vertical Datum of 1988 (NAVD88). Here, we use the convention that the bathymetry is positive, i.e., dry land, above NAVD88.

2. Modeling methodology

The governing model for the circulation of coastal water are the shallow water equations, which are transient and nonlinear partial differential equations [13]. These equations in conservative form are:

Find $(\zeta, \mathbf{u})$ such that:

$$\begin{aligned}
&\frac{\partial \zeta}{\partial t} + div(H\mathbf{u}) = 0, \text{ in } \Omega,\\
&\frac{\partial (Hu_x)}{\partial t} + div\left(Hu_x^2 + \tfrac{g}{2}(H^2 - h_b^2), Hu_xu_y\right) - g\zeta\frac{\partial h_b}{\partial x} = F_x, \text{ in } \Omega,\\
&\frac{\partial (Hu_y)}{\partial t} + div\left(Hu_xu_y, Hu_y^2 + \tfrac{g}{2}(H^2 - h_b^2)\right) - g\zeta\frac{\partial h_b}{\partial y} = F_y, \text{ in } \Omega,
\end{aligned} \tag{1}$$

where ζ is the surface elevation above NAVD88, h_b the bathymetry, $H = \zeta + h_b$ is the total water column, $\mathbf{u} = \{u_x, u_y\}^{\mathrm{T}}$ is the depth

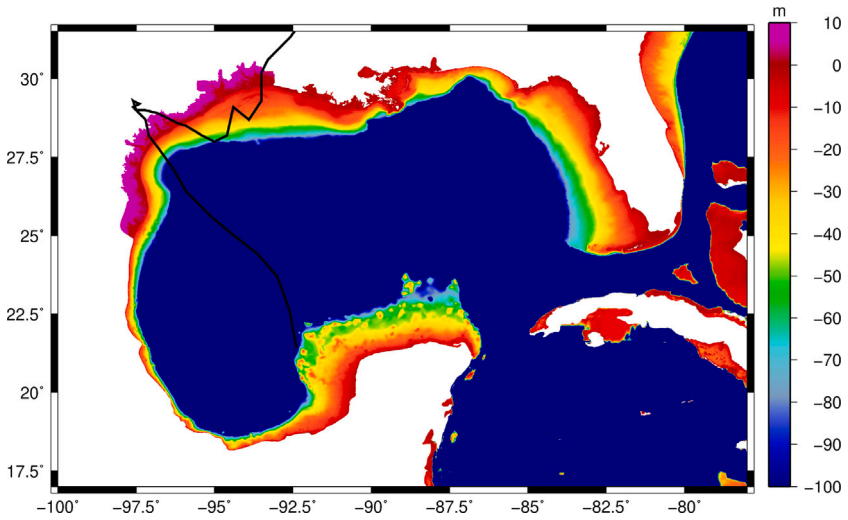

Fig. 5. Track of Hurricane Harvey in the Western Gulf of Mexico from National Hurricane Center Best track data.

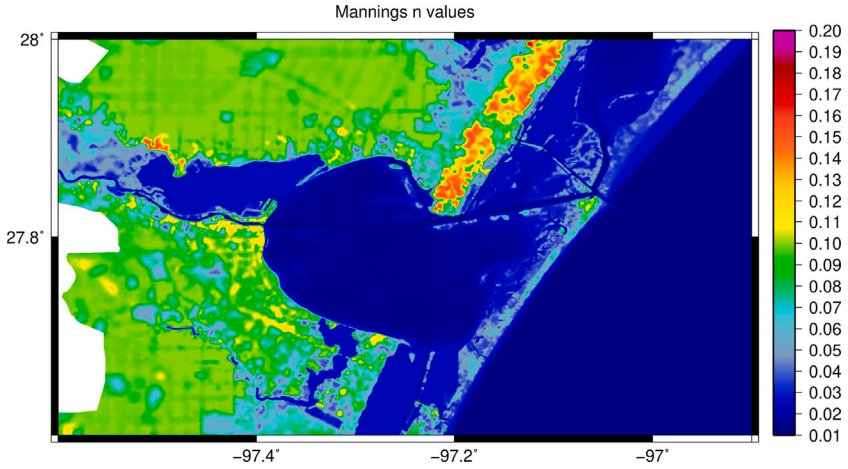

Fig. 6. Manning's n values in the area of interest.

averaged velocity field, and the source terms F_x, F_y represent potential relevant sources which induce flow, including: Coriolis force, tidal potential forces, wind stresses, and wave radiation stresses, as well as potential viscous effects. Finally, Ω is the computational domain. The solution of these equations over physical domains of interest in this case requires the use of numerical approximations. To model storm surge near Aransas Pass due to our hurricanes, we use the well established and validated ADCIRC model first introduced in [11]. ADCIRC uses a Bubnov–Galerkin finite element method [14] along with a semi explicit time stepping scheme (all nonlinearities handled explicitly) to solve a flavor of the two-dimensional depth-integrated shallow water Eqs. (1). In particular, the first equation of (1) is modified into a form called the generalized wave continuity equation (GWCE) [15]. ADCIRC is well suited to this application as it uses unstructured meshes that are capable of accurately description of intricate coastal domains. The details of the finite element formulation, the time stepping scheme, and their accuracy within in ADCIRC is beyond the scope of the current application, and we refer interested readers to the report [16], in particular chapters 1 and 2. In addition to the shallow water equations, we also model the effects of wave energy transfer in deep oceans by using ADCIRC coupled to a wave model - simulating waves nearshore (SWAN). SWAN is a phase-averaged wave model based on the action balance equation [17]:

$$\begin{aligned} \frac{\partial N}{\partial t} + \nabla \cdot (\mathbf{c}N) = \frac{S(N,x,y,\sigma,\theta,t)}{\sigma} \quad &\text{on} \quad \Omega, \\ N = N_{-} \quad &\text{on} \quad \Gamma_{-}, \\ N = N_0 \quad &\text{on} \quad \Omega \quad \text{at} \quad t = 0, \end{aligned} \tag{2}$$

where S denotes the source/sink terms, Ω the computational domain, and N_{-} the specified essential boundary condition on the outflow boundary. The dependence of S on $(N, x, y, \sigma, \theta, t)$ reveals that this is a nonlinear, five-dimensional equation. The solution of (2) in SWAN is accomplished using low order finite difference methods. SWAN was coupled tightly with ADCIRC in 2011 and is described in detail in [18]. These wave effects can lead to significant impact on storm surge magnitude and are therefore included here. ADCIRC+SWAN solves for wave–current interaction during hurricanes and is used in hurricane forecasting and hindcasting, and is the basis of a real-time storm surge forecast system. To make the computations of ADCIRC+SWAN tractable, we use supercomputers at the Texas Advanced Computing Center (TACC). ADCIRC+SWAN is parallelized based on domain decomposition and the MPI (Message Passing Interface) library and the parallelization details along with scaling studies are in [19]. The parallel performance of this code has been documented in several publications and we refer to [20] for further details.

The impacts of the deepened channel bathymetry are assessed by development of two distinctive ADCIRC+SWAN models based on

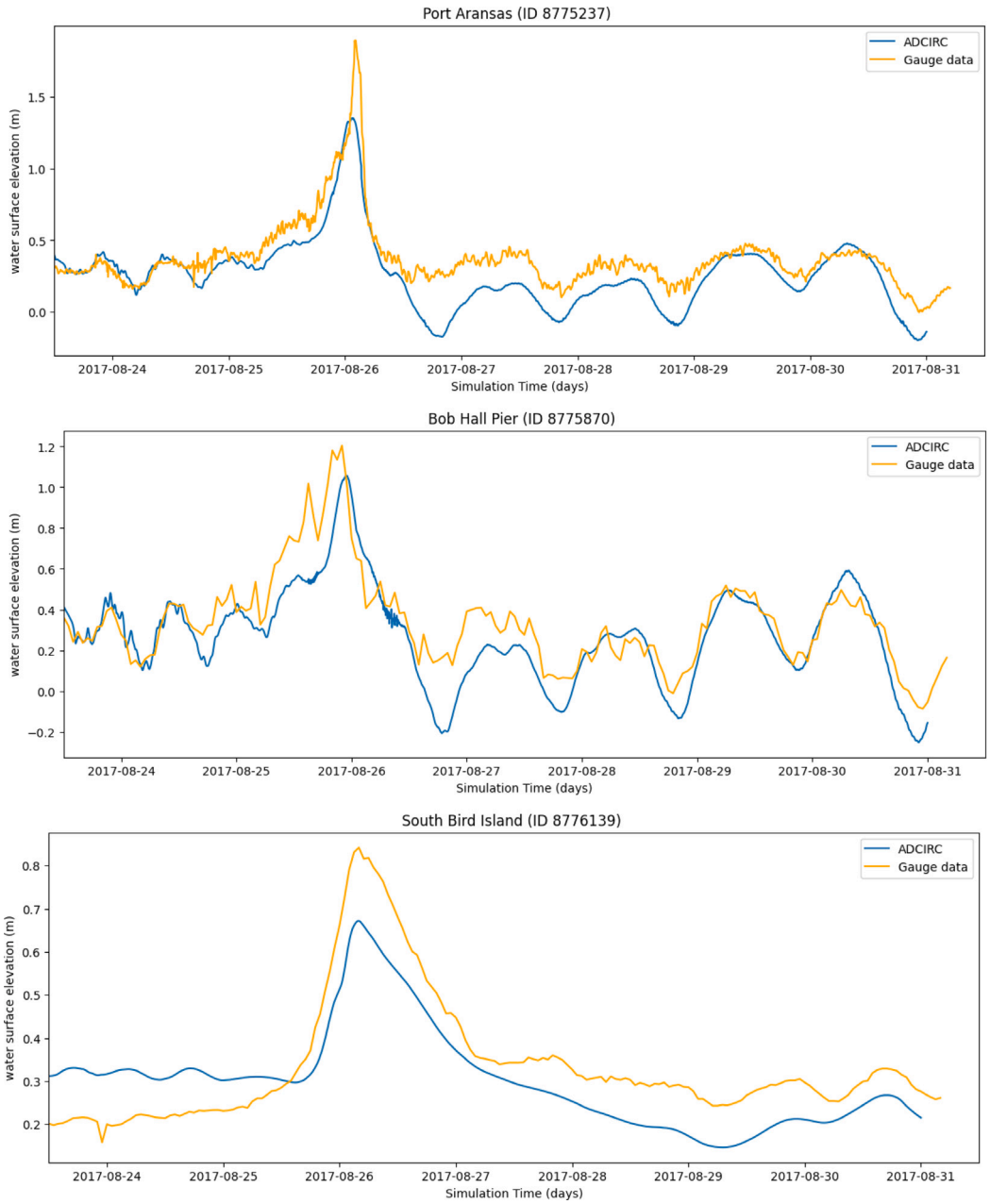

Fig. 7. Comparison of ADCIRC outputs and measured gauge data.

two different finite element meshes. These meshes differ only on the bathymetry in the ship channel and are otherwise identical. The bathymetry of the current and proposed channels are shown in Fig. 3. The resolution of the unstructured finite element meshes varies from an order of kilometers in the deep ocean down to a few dozen meter on the Texas coast and floodplains. Currently, the mesh is used in operational hurricane storm surge forecasting on the coast of Texas and has been extensively validated through fore- and hindcasting of tides and hurricanes, see [21]. The development of the mesh used in the present study is described in Section 2.2 of [21]. The mesh and its extent into the North Atlantic and Gulf of Mexico is shown in Fig. 4. The mesh extends inland from the coastline to a contour approximately 10m above NAVD88. To accurately model the effects of coastal protection systems, the mesh resolves the size of jetties and contains a description of levees and seawalls, and uses a weir formula to assess overtopping of these, see [22]. Finally, to capture the critical process of inundation, overwash, and flow over land, ADCIRC has an advanced algorithm for wetting and drying of the finite elements [23] in the mesh.

In our previous study, [2] we validated the current channel configuration with recent gauge data. In [4], the mesh was also used for Hurricane Harvey and we exactly mimic their setup for the current models and validate its results below.

2.1. ADCIRC model set-up

Prior to landfall on August 25th 2017 on San José island (approximately 25km northeast of the Aransas Pass), the storm system that lead to Hurricane Harvey initially formed in the Atlantic Ocean in the middle of August 2017 [24], see, Fig. 5 for its track in the Western Gulf of Mexico.

After landfall, the storm system moved back into The Gulf and subsequently moved northeast and lead to extreme rainfall in Houston and surrounding areas.

In addition to a mesh as presented in the preceding section, the ADCIRC+SWAN model requires tides and meteorological data to induce

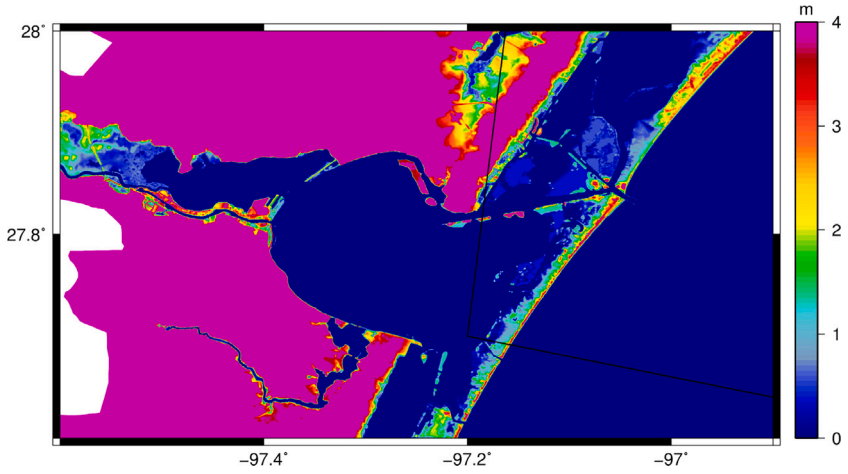

Fig. 8. Synthetic hurricane track.

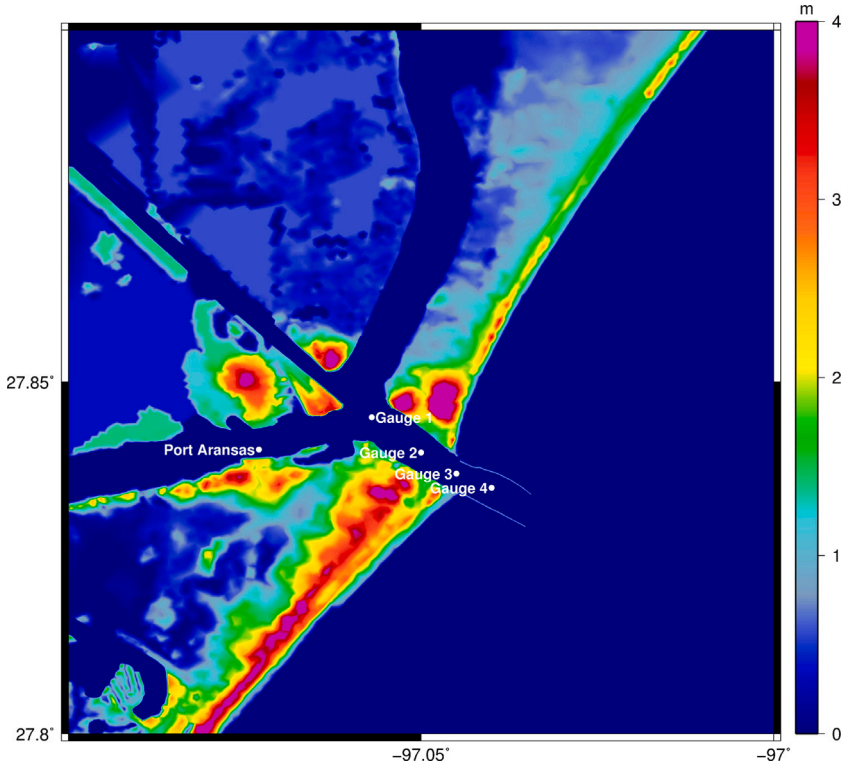

Fig. 9. NOAA gauge Port Aransas and synthetic elevation gauges in Aransas Pass.

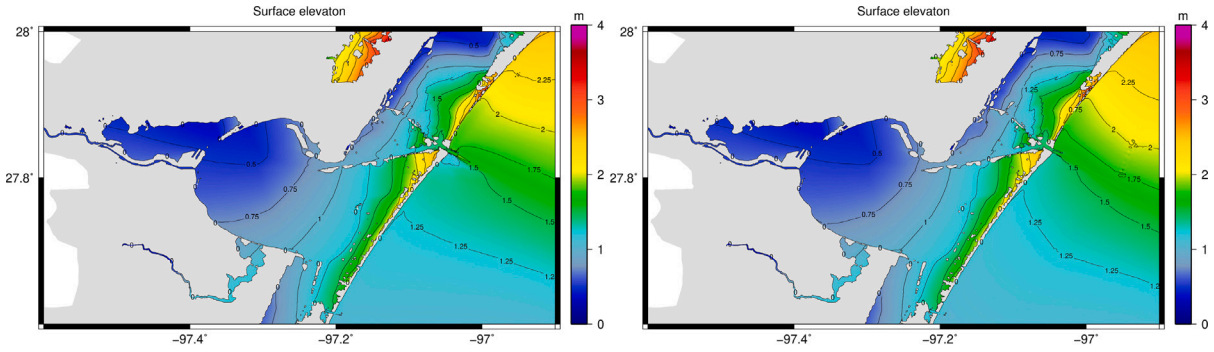

Fig. 10. Maximum storm surge (in meters) in the region of interest.

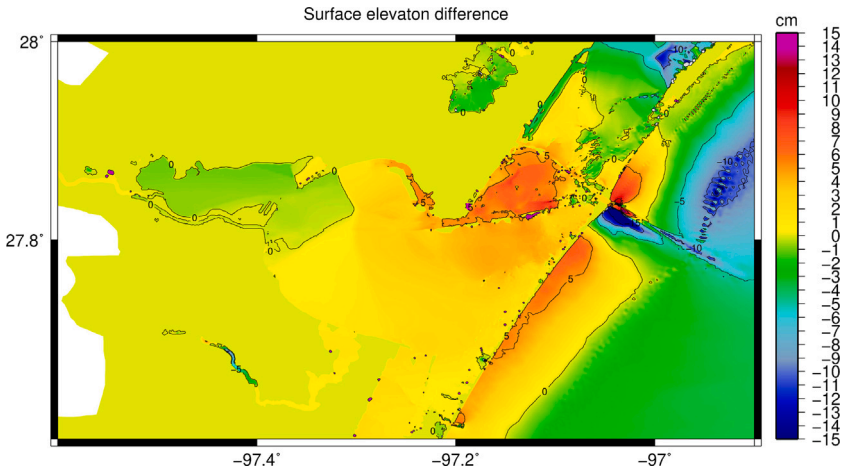

Fig. 11. Maximum storm surge difference (in centimeters) in the region of interest.

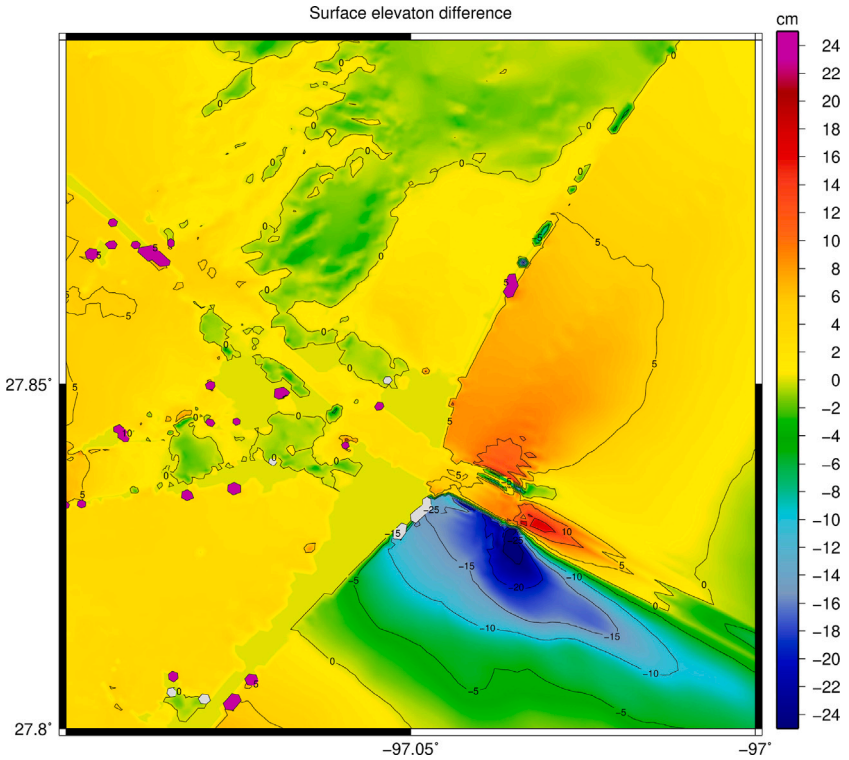

Fig. 12. Maximum storm surge difference (in centimeters) in the Aransas Pass.

circulation and subsequent storm surge. The tides are obtained with OceanMesh2D [25], which in turn utilizes the TPXO9 tidal model [26] to define a periodic forcing based on the Q1, O1, P1, K1, N2, M2, S2, and K2 tidal constituents. Additionally, tidal we apply a elevation condition corresponding to these tides applied along the 60° meridian, the far eastern portion shown in Fig. 4. At the portion of the mesh furthest inland, we apply a no-normal flow boundary condition to ensure solvability of the system of equations.

Meteorological data corresponding to hurricane wind and pressure fields are incorporated into the ADCIRC+SWAN model by using parametric hurricane model, the Generalized Asymmetric Holland Model (GAHM). This parametric model is based on the classical Holland Model (HM) [27] and has been specifically developed for ADCIRC hurricane models. These parametric models use National Hurricane Center forecasts (or hindcasts after the hurricanes have passed) which includes time series data such as storm track, central pressure, maximum winds, *etc.* In this study, we use the best track information determined by the National Hurricane Center. The classical HM produces an idealistic symmetric hurricane which is less applicable to forecasting of hurricane storm surge, and an asymmetric HM was developed in [28]. This asymmetric was further improved for forecasting with ADCIRC, particularly for large hurricanes affected by Coriolis forces. We refer to the ADCIRC Wiki page *https://wiki.adcirc.org/Generalized_Asymmetric_Holland_Model#cite_note-1* for further details on the GAHM. Additionally, momentum is transferred from the hurricane wind and pressure fields to the seawater by a wind drag coefficient, see [29,30] and the reduction of these fields over land are considered with surface roughness, see [31]. In (1), the momentum transfer is part of the right hand side of the momentum equations within F_x, F_y.

In addition to meteorological and tidal forcings, our ADCIRC mesh contains a description of the roughness of land and sea bottoms through a spatially variable Manning's n value. The Manning's values are used

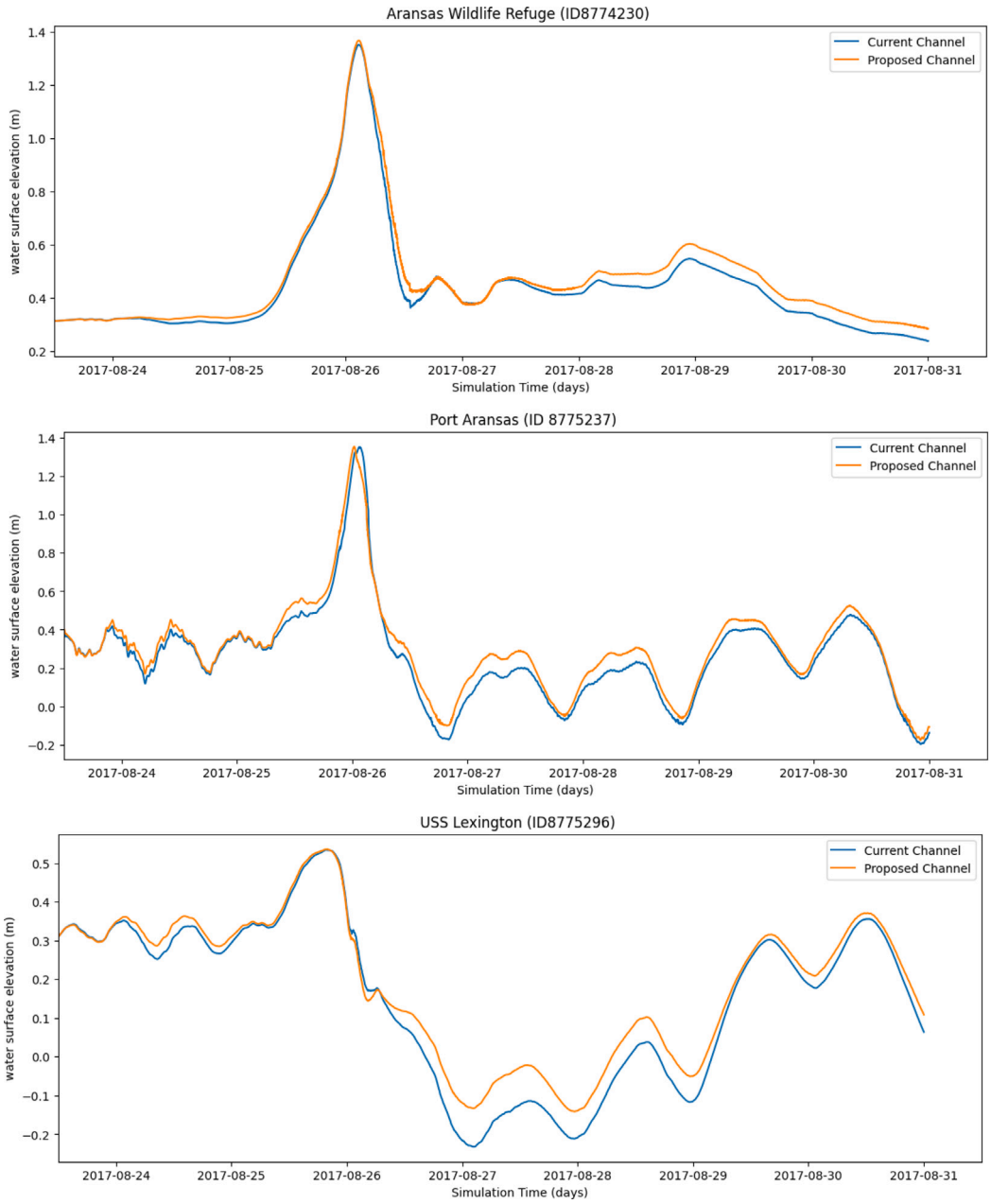

Fig. 13. Comparison of ADCIRC output hydrographs (in meters) at selected gauges.

to ascertain hydraulic friction and the Manning's n values are assigned based on the NOAA land cover database *Coastal Change Analysis Program*, see *https://coast.noaa.gov/digitalcoast/data/ccapregional.html*. The classification of Manning's n values from databases are presented in [30]. In Fig. 6, the Manning's n values in the region of interest are shown. For the two different meshes with different channels, we use the same Manning's n values and changes in bottom friction are accounted for by changed friction due to change in water column depth.

To ensure accuracy and numerical stability of our ADCIRC+SWAN model, we follow the approach laid out in [4], where a two-step model run was performed. First, an ADCIRC only run without meteorological forcing is performed for the 21 day time period before our best track hurricane data starts. This tidal "spin-up" is subsequently used as an initial condition for a full ADCIRC+SWAN run forced with tides and meteorological data which covers the period from noon August 23rd to noon August 31st. As the channel is narrow, we expect advective effects will impact the flows significantly during a hurricane and we depart from the approach in [4] by including all advective acceleration terms found in the GWCE. Hence, we have reduced the time step to 0.1 s from the 1 second used previously in modeling efforts for Hurricane Harvey using ADCIRC.

2.2. Model validation

As there has been updates to the ADCIRC codebase since the efforts in [4], we perform a brief model validation. To this end, we compare model outputs for the case of the current channel depth to NOAA gauge data in the area north and south of Aransas Pass. In Fig. 7, these comparisons are presented for three NOAA gauges: Port Aransas (ID 8775237), Bob Hall Pier (ID 8775870), and Aransas Wildlife Refuge (ID 8774230).

The first gauge is also used in Figure 3 of [4], and the ADCIRC results are identical from visual inspection. Hence, we conclude that the model for the current channel is able to reproduce the same

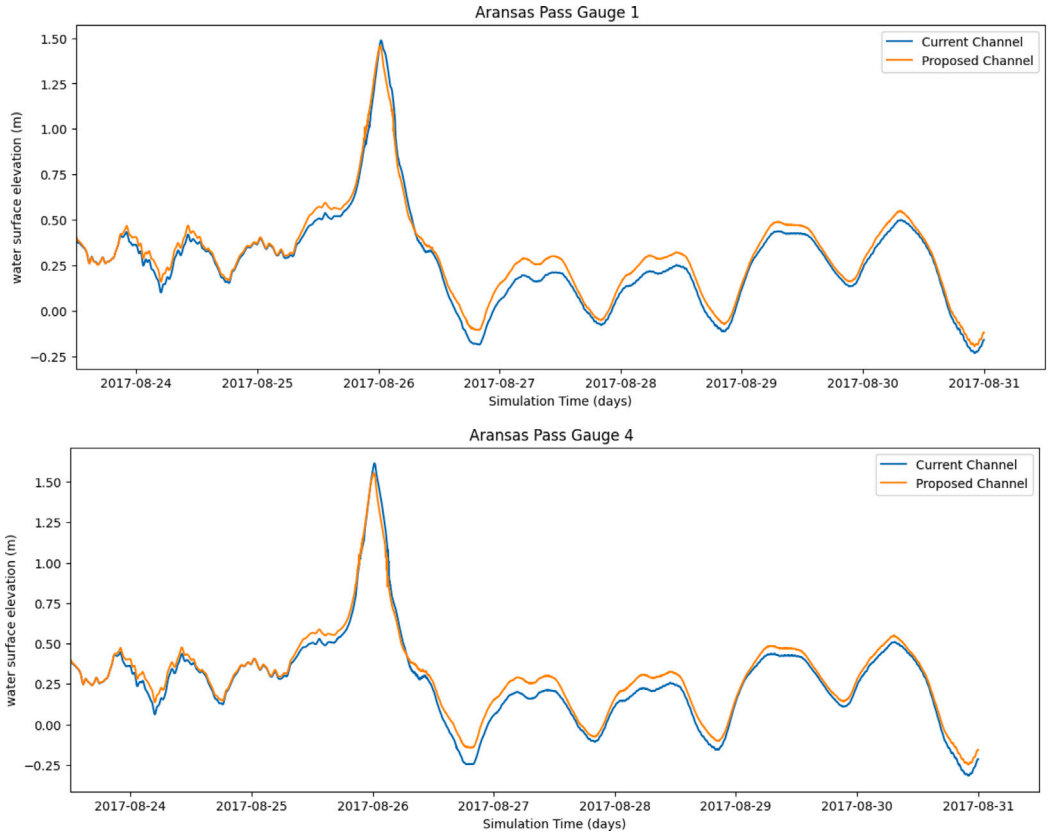

Fig. 14. Comparison of ADCIRC output hydrographs (in meters) at synthetic gauges.

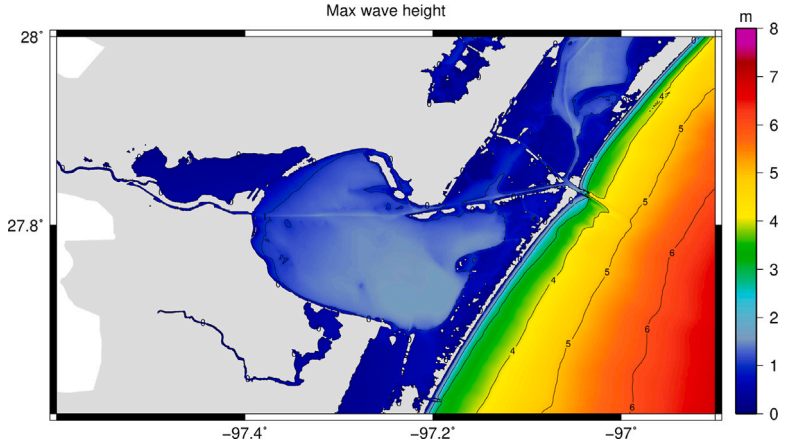

Fig. 15. Maximum significant wave height during Hurricane Harvey (in meters).

results as [4]. The model results agree very well at the Bob Hall Pier Gauge, whereas at the Aransas Wildlife Refuge gauge and the gauge in Port Aransas, ADCIRC underpredicts the peak surge. We expect this is partly due to the position of this gauge and the effects of erosion and morphodynamics during Hurricane Harvey (see [4] for further details).

The ADCIRC outputs in Fig. 7 are identical to those presented in [4] for the same gauges. However, as noted above the results are not a perfect match with the gauge data. While the parametric hurricane model GAHM provides a representation of a hurricane particularly useful for forecasting it was developed using several simplifying considerations. High resolution validated data-assimilated forcings from commercial providers, such as those used for Hurricane Ike in [21], generally leads to higher accuracy. However, for the comparisons performed in present study we consider the parametric hurricane models to be sufficient.

3. Results

To qualitatively assess the effects of the proposed channel depth on hurricane storm surge, we analyze the ADCIRC+SWAN model outputs. To this end, we consider both maximum surge magnitude in the study area as well as hydrographs of the water surface elevation at existing gauge locations. This will allow us to assess the effects onto both timing and magnitude of storm surge. We compare the ADCIRC+SWAN outputs of maximum elevation as well as elevation time series at selected locations near Aransas Pass. In addition to these water surface

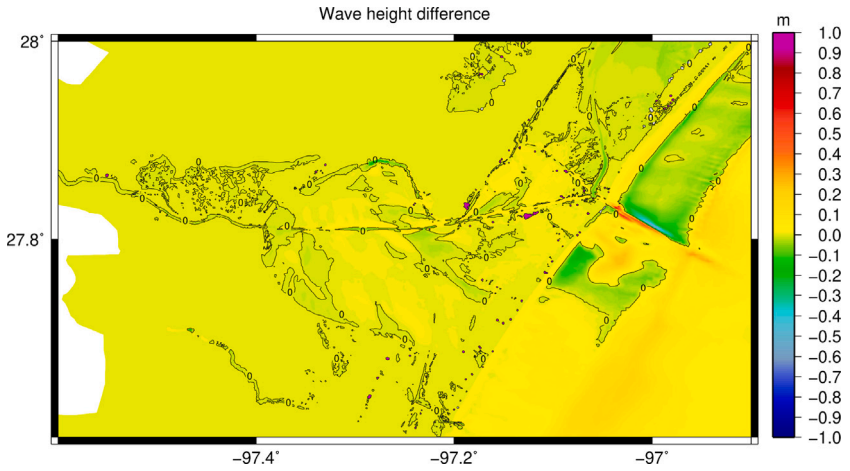

Fig. 16. Difference in maximum significant wave height (in meters) between current and proposed channel depths.

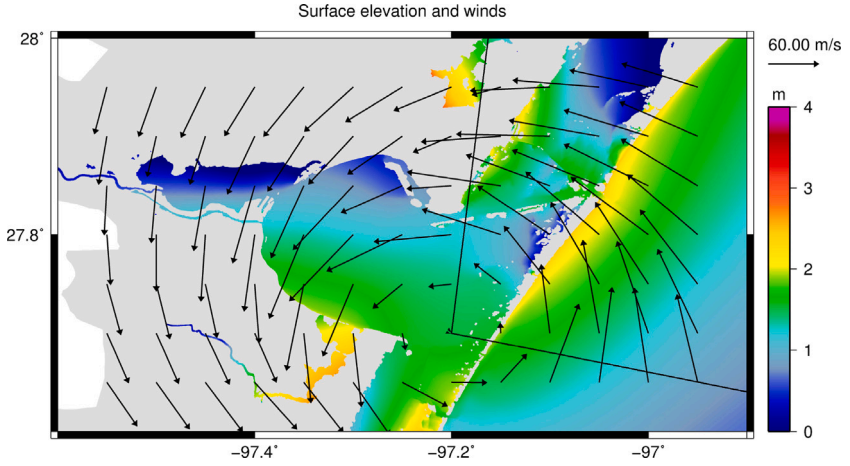

Fig. 17. Water surface elevations (in meters) and wind vectors in the region of interest at the time of landfall.

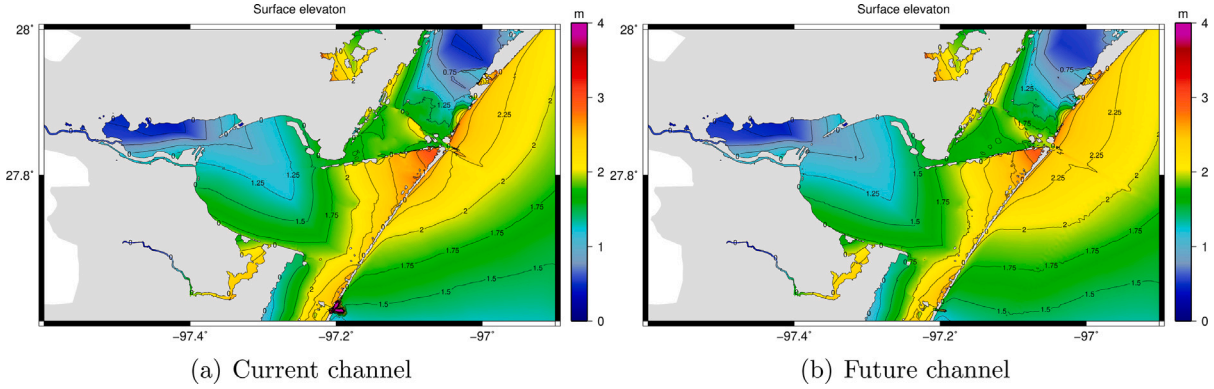

Fig. 18. Maximum storm surge (in meters) in the region of interest.

elevation outputs, we also compare the changes in significant wave height [32], as the effects of waves can lead to significant damage of coastal structures. In particular, we consider a hindcast of Hurricane Harvey based on its best track data as well as a synthesized derived version. The synthetic version employs the same GAHM hurricane model as Harvey, however, the track of the storm is shifted. Hurricane Harvey resulted in significant alongshore winds in this study area and as noted in [4], these winds lead to storm surge behind the barrier islands within the Corpus Christi Bay estuarine system. We therefore consider a synthesized hurricane track where the eye is shifted in a southwestern direction such that the maximum winds perpendicular to the shore pass through the Aransas Pass. In Fig. 8, the shifted hurricane track is shown in the study area as the black solid line.

We consider the following National Oceanic and Atmospheric Administration (NOAA) gauges (see *https://tidesandcurrents.noaa.gov* for further details) in the study area: "Aransas Wildlife Refuge" (ID 87742 30), "Port Aransas" (ID 8775237), and "USS Lexington" (ID 8775296). In addition to these NOAA gauges, we consider elevation time series data at artificial gauges in Aransas pass (Fig. 9).

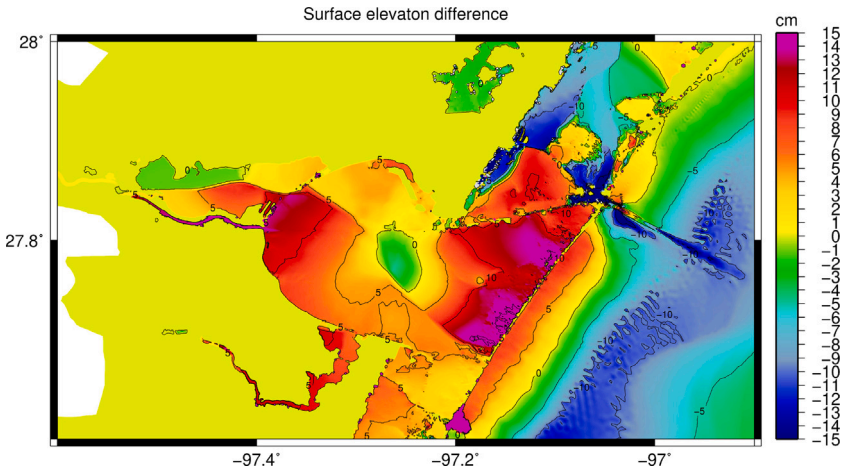

Fig. 19. Maximum storm surge difference (in centimeters) in the region of interest.

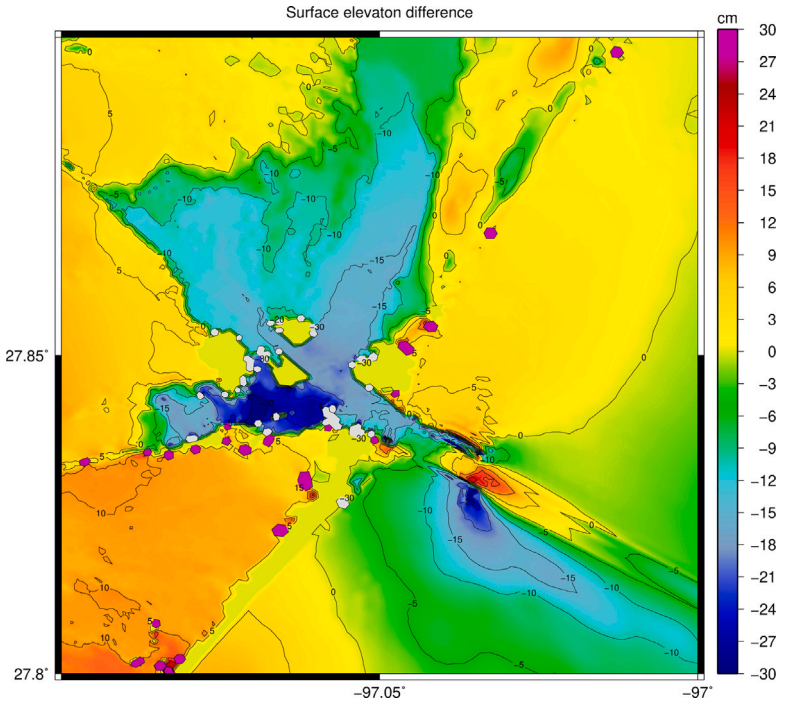

Fig. 20. Maximum storm surge difference (in centimeters) in the Aransas Pass.

3.1. Hurricane Harvey

The track of Hurricane Harvey was such that it made landfall approximately 25km north of the Aransas Pass Channel. This lead to significant surge from both on- and alongshore winds in the area near the City of Port Aransas. In Fig. 10(a), the ADCIRC+SWAN maximum elevation model outputs are shown corresponding to the current channel for the best track Hurricane Harvey forcing data. In Fig. 10(b), an identical forcing scenario is shown for the proposed channel bathymetry. Inspection of the maximum surge in Figs. 10(a) and 10(b) reveal significant surge in the area for both channel depths. To further visually analyze these results, we present Figs. 11 and 12, where the difference in maximum surge are shown. In these two figures the difference between the current and proposed channel depth maximum surge in centimeters are shown. Hence, negative numbers indicate increased maximum surge with the proposed channel. The differences presented in Fig. 11 show that in most of the area the model results do not suggest a significant change in surge. However, as shown in Fig. 12, the model results suggest that the area immediately south of the southern jetty does experience an increase up to 25 centimeter. Furthermore, in the bays inside Aransas Pass the model results indicate a slight decrease in peak surge in large portions with some northern areas indicating small increases of a few centimeters. This observed increase is possibly due to the increased capability of the deeper channel to accommodate the flow from the surge in the bays behind the barrier island during Hurricane Harvey. Some of the additional flow through the Aransas Pass may in this case route in a northern direction in the Lydia Ann Channel, the northern split inside Aransas Pass shown in Fig. 9.

To present a time series of water surface elevation at gauges in the region we use the ADCIRC output at locations of NOAA gauges in the vicinity of Aransas Pass. Due to similar results of the synthetic gauges in the Aransas Pass, we only present hydrographs of gauges 1 and 4. In Figs. 13 and 14, these hydrographs are presented and each plot is followed by the difference between the hydrograph of the current channel versus the proposed channel. The observations from the visual

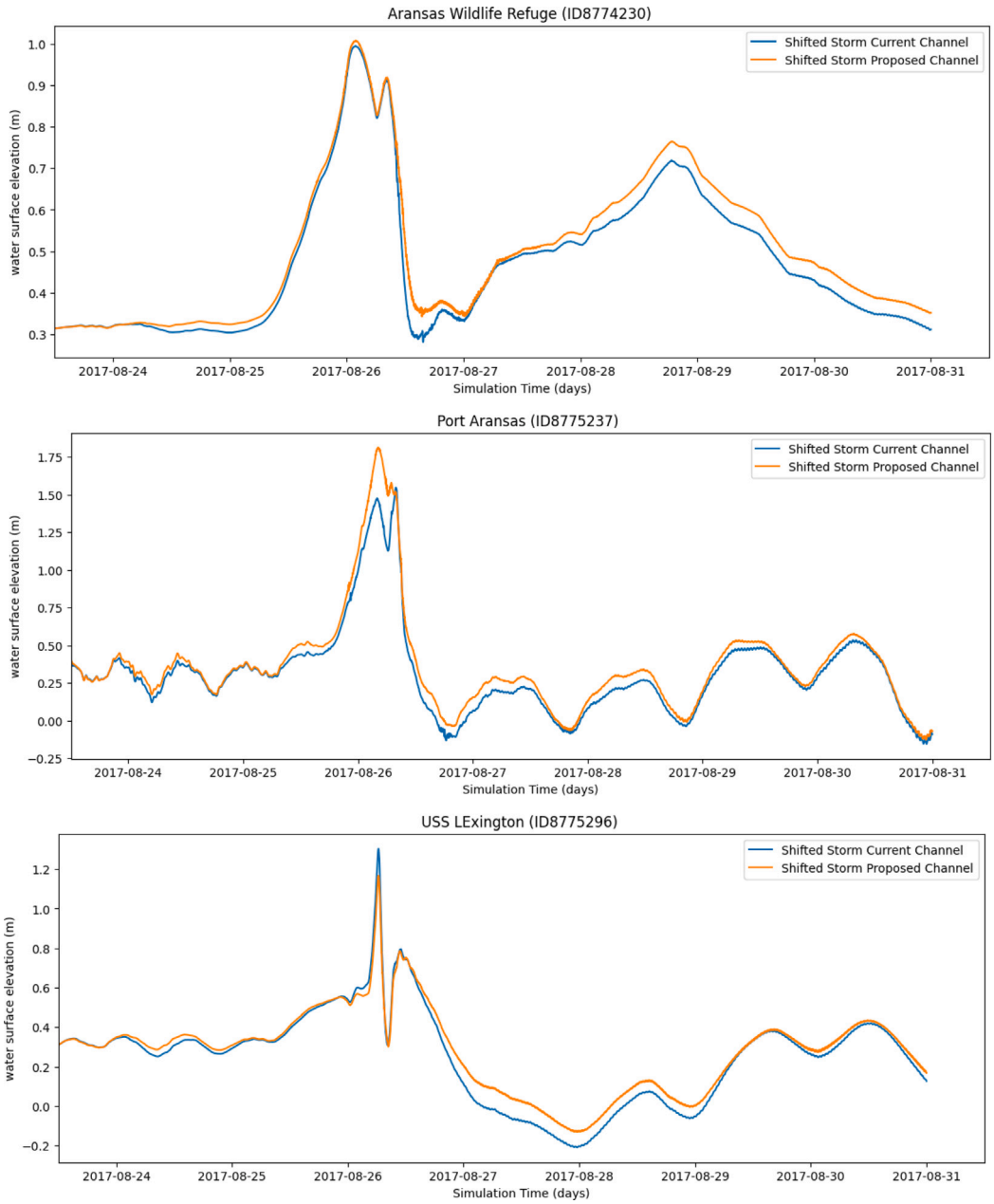

Fig. 21. Comparison of ADCIRC output hydrographs (in meters) at selected gauges.

representation of maximum surge elevation and the corresponding difference in the region are mirrored in these hydrographs. Hence, all hydrographs see a reduced maximum surge with the exception of "Aransas Wildlife Refuge" which is located north of Port Aransas where a modest increase in maximum surge is observed. We also note that after the maximum surge has receded, the deeper channel case sees increased water levels in some locations shown in Figs. 13 and 14.

The final comparison we make between the current and proposed channel is for the maximum significant wave height (see [32]). In Fig. 15, the maximum significant wave height is shown. Correspondingly, in Fig. 16, the difference in the significant wave height between the two channel depths is shown. The difference between the two channels is negligibly small in most of the region but at the entrance of Aransas Pass, a significant decrease is observed along with a small increase near the north jetty. A minor increase of up to 0.2m is also seen in the area surrounding the jetties and in the area north of the jetties. Overall, the figure shows that the differences in significant wave height are minor from our model results.

3.2. Synthetic Hurricane Harvey

To further investigate the effects of a deeper channel in response to a storm of intensity and magnitude of Hurricane Harvey, we now consider the case shown in Fig. 17. In particular, we consider a case where the eye of the hurricane passes to the south of the City of Port Aransas and thus ensure that the maximum winds directed towards the shore passes through Aransas Pass. This storm characteristic will lead to significant surge in the Aransas Pass and on the shore near the Corpus Christi Ship Channel. The maximum surge for the current and proposed channels are shown in Figs. 18(a) and 18(b). The interaction of surge from both winds along and towards the shore lead to a prediction of surges of more than 3 meters for both channel depths.

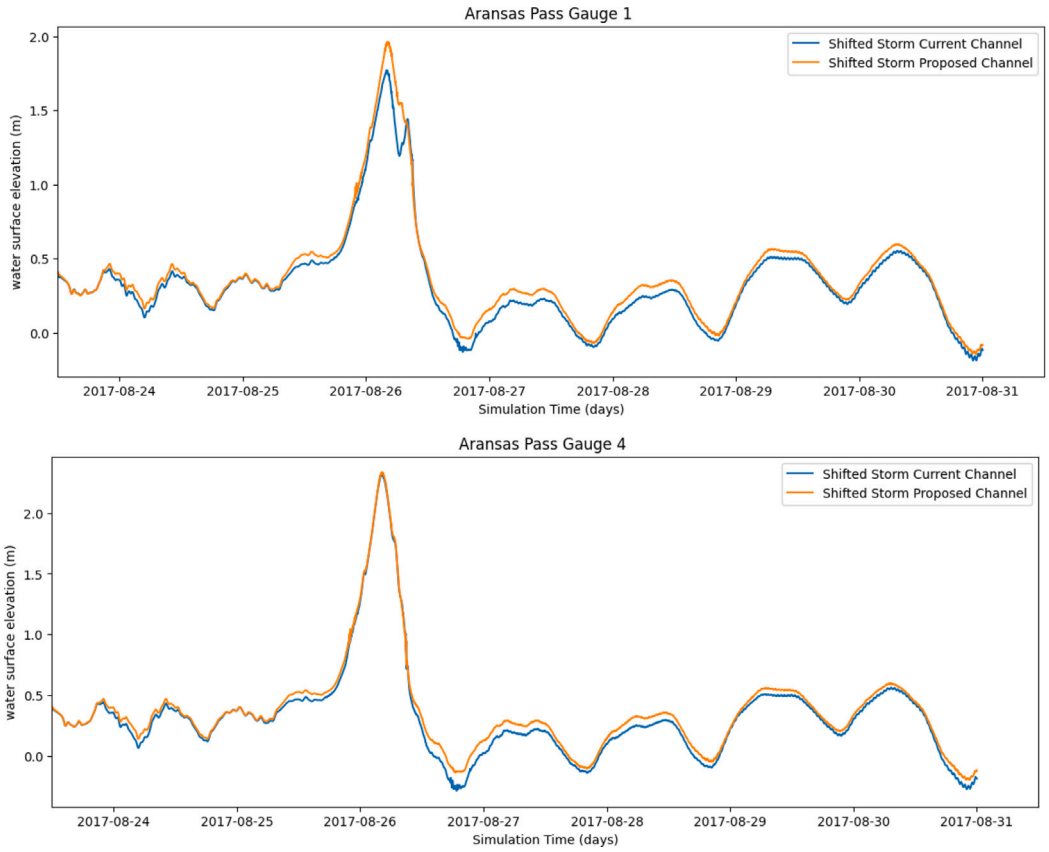

Fig. 22. Comparison of ADCIRC output hydrographs (in meters) at synthetic gauges.

The trajectory of this synthetic hurricane leads to significant surge within Corpus Christi Bay, the Aransas Pass, and in Port Aransas as shown in Fig. 18(a). Comparison of the maximum surge in Figs. 18(a) and 18(b) shows a significant difference in the locations and magnitudes of maximum surge. We note in particular the significant reduction of maximum surge throughout Corpus Christi Bay and on the inside of the barrier islands. To highlight these differences we also present figures where the difference between the maximum surge of the current versus the proposed channel depths are shown. Fig. 19 shows this difference for the region and Fig. 20 shows the difference near Port Aransas. The difference in maximum surge between the two channels follows a similar trend as Hurricane Harvey in Corpus Christi Bay and along the ship channel. However, close to Aransas Pass and Port Aransas, we observe an increase in the maximum surge of up to 30 centimeter.

Finally, we present the hydrographs at selected locations in Figs. 21 and 22. The observations from these are similar to the previous case and we observe no clear trend across these hydrographs other than that the storm surge does not significantly change at its peak for these gauge locations. At the Aransas Wildlife Refuge gauge, the maximum storm surge is slightly increased for the proposed channel. Whereas at the Port Aransas gauge, an increase of approximately 30 centimeters is observed as well as a different post peak surge response. At the USS Lexington in Corpus Christi, the deeper channel leads to a reduced peak surge. Synthetic gauge 1 in Aransas Pass sees an increase in surge, whereas gauge 4 exhibits the converse, though with very small difference, as seen in Fig. 22. This effect is also observed in Fig. 20, where the portions of the pass near the ocean exhibits a reduction in maximum surge and the inland portions of the pass sees the converse.

We again assess the difference in maximum significant wave height. In Fig. 23, the difference in the significant wave height is shown. We again observe distinctive areas near the jetties with increases and decreases in maximum significant wave height up to 1 meter and observe approximately a 10 centimeter increase along the ship channel.

4. Concluding remarks

The development of infrastructure in coastal regions can impact the balance and interaction between linked human-natural systems. Furthermore, the uncertainty within these interactions as well as in their links require scientific consideration to understand the risk of infrastructure developments on these linked systems. In the case of the Corpus Christi Ship Channel, more information about the potential impacts of a deeper channel to accommodate large crude oil tankers on hurricane storm surge was needed. The ship channel is the only connection between the coastal ocean and the estuaries and bays behind the barrier islands for tens of miles to the north and south of the Aransas Pass. In a previous paper [2], we studied the impacts on the recruitment of estuarine dependent Red drum fish larvae and found negligible small impacts. Another potentially severe impact of a deepened channel is on hurricane storm surge magnitude and extent. In the nearby cities and counties, there is significant critical infrastructure (e.g., the Port of Corpus Christi) and a few hundred thousand inhabitants. Hence, changes to storm surge in this region can have significant human and economical impacts.

To study the impacts of the deepened ship channel, we have developed two models governing the coastal hydrodynamics an hurricane storm surge in the region of interest. The models are used to ascertain hurricane storm surge using winds from Hurricane Harvey as well as a synthetic storm for the current and proposed channel bathymetries. From the model outputs for these cases, we analyze the outputs with a focus on changes to maximum storm surge magnitude as well as hydrograph time series at elevation gauge locations in the study area. Our model results (in particular the difference in max elevation Figs. 11, 12, 19, 20) overall suggest a reduction in maximum surge in large parts of the study area. However, for the second synthetic storm, our model results indicate an increased surge of approximately 30 centimeter near the Aransas Pass as shown in Fig. 20. We also

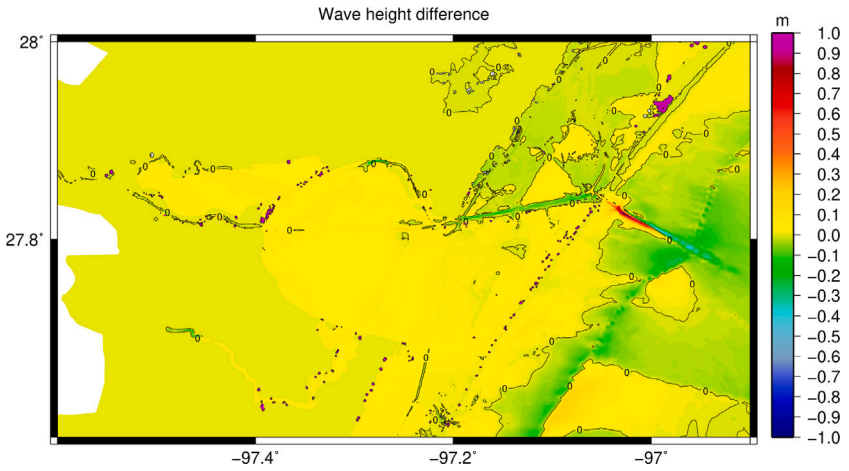

Fig. 23. Difference in maximum significant wave height (in meters) between current and proposed channel depths for the second synthetic version of Hurricane Harvey.

consider the impacts of a deeper channel on significant wave height in the study area. The conclusions we draw here are similar to the storm surge case. However, there are areas near the jetties at the ship channel entrance where the changes in significant wave height are nearly one meter.

While the ADCIRC model and mesh used in this study are extensively validated for storm surge and coastal circulation, there are other physical processes that can impact storm surge. In particular, morphodynamic effects and their impact should be considered in future studies. Furthermore, other storms with different characteristics could also be considered.

Declaration of competing interest

The authors declare that they have no known competing financial interests or personal relationships that could have appeared to influence the work reported in this paper.

Data availability

Data will be made available on request

Acknowledgments

The present study was conceived of and initiated by scientists at the University of Texas Marine Science Institute and carried out by faculty and staff from the Oden Institute for Computational Engineering and Sciences of the University of Texas at Austin. Funding provided by the Marine Science Institute included generous contributions made by members of the University of Texas Marine Science Advisory Council, in response to a special request for funds. The authors also gratefully acknowledge the computational resources provided by the Texas Advanced Computing Center and the Frontera supercomputer under allocations “ADCIRC” and “DMS21031”. The authors have no relevant financial or non-financial interests to disclose.

Supplementary information

This article has a corresponding report available from the University of Texas at Austin Marine Science Institute library:

https://utmsi.utexas.edu/images/MSI/Blog_Research/Valseth_and_Dawson_2022.pdf

References

[1] P. Hamilton, E. Wood, L. Lin, T. Campbell, L. Olson, S. Jones, S. Howard, K. Skalbeck, Alternatives to Manage Sediment at the Intersection of the Gulf Intracoastal Waterway and the Corpus Christi Ship Channel, Tech. Rep., ENGINEER RESEARCH AND DEVELOPMENT CENTER VICKSBURG United States, 2018.

[2] E. Valseth, M.D. Loveland, C. Dawson, E.J. Buskey, A study of the potential impact of dredging the Corpus Christi Ship Channel on passive particle transport, J. Mar. Sci. Eng. 9 (9) (2021) 935.

[3] A.E. Frey, F. Olivera, J.L. Irish, L.M. Dunkin, J.M. Kaihatu, C.M. Ferreira, B.L. Edge, Potential impact of climate change on hurricane flooding inundation, population affected and property damages in Corpus Christi 1, JAWRA J. Am. Water Resour. Assoc. 46 (5) (2010) 1049–1059.

[4] J.A. Goff, J.M. Swartz, S.P. Gulick, C.N. Dawson, A.R. de Alegria-Arzaburu, An outflow event on the left side of hurricane Harvey: Erosion of barrier sand and seaward transport through Aransas Pass, Texas, Geomorphology 334 (2019) 44–57.

[5] D. Van Maren, T. van Kessel, K. Cronin, L. Sittoni, The impact of channel deepening and dredging on estuarine sediment concentration, Cont. Shelf Res. 95 (2015) 1–14.

[6] K.K. Venancio, P.D. Garcia, T.Z. Gireli, T.B. CORRêA, Hydrodynamic modeling with scenario approach in the evaluation of dredging impacts on coastal erosion in Santos (Brazil), Ocean Coast. Manag. 195 (2020) 105227.

[7] M.V. Bilskie, Hydrodynamic modeling of tides and hurricane storm surge for pre-and post-dredging conditions in the lower St. Johns River, Florida, in: Ports 2013: Success Through Diversification, 2013, pp. 1955–1964.

[8] R. Familkhalili, S.A. Talke, The effect of channel deepening on tides and storm surge: A case study of Wilmington, NC, Geophys. Res. Lett. 43 (17) (2016) 9138–9147.

[9] R. Familkhalili, S.A. Talke, D.A. Jay, Tide-storm surge interactions in highly altered estuaries: How channel deepening increases surge vulnerability, J. Geophys. Res.: Oceans 125 (4) (2020) e2019JC015286.

[10] S.A. Talke, R. Familkhalili, D.A. Jay, The influence of channel deepening on tides, river discharge effects, and storm surge, J. Geophys. Res.: Oceans 126 (5) (2021) e2020JC016328.

[11] R.A. Luettich, J.J. Westerink, N.W. Scheffner, et al., ADCIRC: An advanced three-dimensional circulation model for shelves, coasts, and estuaries. Report 1, theory and methodology of ADCIRC-2DD1 and ADCIRC-3DL, 1992.

[12] J. Roelvink, G. Van Banning, Design and development of DELFT3D and application to coastal morphodynamics, Oceanograph. Lit. Rev. 11 (42) (1995) 925.

[13] W.-Y. Tan, Shallow Water Hydrodynamics: Mathematical Theory and Numerical Solution for a Two-Dimensional System of Shallow-Water Equations, Elsevier, 1992.

[14] T.J. Hughes, The Finite Element Method: Linear Static and Dynamic Finite Element Analysis, Courier Corporation, 2012.

[15] D.R. Lynch, W.G. Gray, A wave equation model for finite element tidal computations, Comput. & Fluids 7 (3) (1979) 207–228.

[16] R.A. Luettich, J.J. Westerink, Formulation and Numerical Implementation of the 2D/3D ADCIRC Finite Element Model Version 44. XX, Vol. 20, R. Luettich Chapel Hill, NC, USA, 2004.

[17] N. Booij, L.H. Holthuijsen, R.C. Ris, SWAN wave model for shallow water, in: Proceedings of the 1996 25th International Conference on Coastal Engineering, ASCE, Vol. 1, 1996, pp. 668–676.

[18] J.C. Dietrich, M. Zijlema, J.J. Westerink, L.H. Holthuijsen, C.N. Dawson, R.A. Luettich, R.E. Jensen, J.M. Smith, G.S. Stelling, G.W. Stone, Modeling hurricane waves and storm surge using integrally-coupled, scalable computations, Coast. Eng. 58 (2011) 45–65.
[19] S. Tanaka, S. Bunya, J.J. Westerink, C.N. Dawson, R.A. Luettich, Scalability of an unstructured grid continuous Galerkin based hurricane storm surge model, J. Sci. Comput. 46 (2011) 329–358.
[20] J.C. Dietrich, S. Tanaka, J.J. Westerink, C.N. Dawson, R.A. Luettich, M. Zijlema, L.H. Holthuijsen, J.M. Smith, L.G. Westerink, H.J. Westerink, Performance of the unstructured-mesh, SWAN+ADCIRC model in computing hurricane waves and surge, J. Sci. Comput. 52 (2012) 468–497.
[21] M.E. Hope, J.J. Westerink, A.B. Kennedy, P. Kerr, J.C. Dietrich, C. Dawson, C.J. Bender, J. Smith, R.E. Jensen, M. Zijlema, et al., Hindcast and validation of Hurricane Ike (2008) waves, forerunner, and storm surge, J. Geophys. Res.: Oceans 118 (9) (2013) 4424–4460.
[22] R. Luettich, J. Westerink, An assessment of flooding and drying techniques for use in the ADCIRC hydrodynamic model: Implementation and performance in one-dimensional flows, 1995, Contract Report, prepared for Headquarters, US Army Corps of Engineers, Vicksburg, MS.
[23] J. Dietrich, R. Kolar, R.A. Luettich, Assessment of ADCIRc's wetting and drying algorithm, in: Developments in Water Science, vol. 55, Elsevier, 2004, pp. 1767–1778.
[24] E. Blake, D. Zelinsky, Hurricane Harvey. National hurricane center tropical cyclone rep. AL092017, 2018.
[25] W. Pringle, OceanMesh2D: User guide - Precise distance-based two-dimensional automated mesh generation toolbox intended for coastal ocean/shallow water, 2018.
[26] G. Egbert, S. Erofeeva, Efficient inverse modeling of barotropic ocean tides, J. Atmos. Ocean. Technol. 19 (2) (2002) 183–204.
[27] G.J. Holland, An analytic model of the wind and pressure profiles in hurricanes, 1980.
[28] C. Mattocks, C. Forbes, L. Ran, Design and Implementation of a Real-Time Storm Surge and Flood Forecasting Capability for the State of North Carolina, UNC-CEP Technical Report 30, 2006.
[29] M.D. Powell, I. Ginis, Drag coefficient distribution and wind speed dependence in tropical cyclones, 2006, Final Report to the National Oceanic and Atmospheric Administration (NOAA) Joint Hurricane Testbed (JHT) Program.
[30] J. Dietrich, J. Westerink, A. Kennedy, J. Smith, R. Jensen, M. Zijlema, L. Holthuijsen, C. Dawson, R. Luettich, M. Powell, et al., Hurricane Gustav (2008) waves and storm surge: Hindcast, synoptic analysis, and validation in Southern Louisiana, Mon. Weather Rev. 139 (8) (2011) 2488–2522.
[31] S. Bunya, J.C. Dietrich, J. Westerink, B. Ebersole, J. Smith, J. Atkinson, R. Jensen, D. Resio, R. Luettich, C. Dawson, et al., A high-resolution coupled riverine flow, tide, wind, wind wave, and storm surge model for southern Louisiana and Mississippi. Part I: Model development and validation, Monthly Weather Rev. 138 (2) (2010) 345–377.
[32] L.H. Holthuijsen, Waves in Oceanic and Coastal Waters, Cambridge University Press, 2007.

Eirik Valseth is an Associate Professor of Scientific Computing at the Norwegian University of Life Science (NMBU) Department of Data Science as well as a research associate at the Oden Institute For Computational Engineering and Sciences at the University of Texas at Austin, and a researcher at Simula Research Laboratory Department of Numerical Analysis and Scientific Computing. Prior to joining NMBU and Simula, Eirik held an individual Marie Skłodowska-Curie Actions project working on finite element methods for multidimensional PDEs. In addition to this, Eirik currently focuses on the development of novel shallow water equation solvers, modeling tools, and techniques for compound flooding and hydropower applications.